

Critical cooling rate and thermal stability of Zr–Ti–Cu–Ni–Be alloys

Theodore A. Waniuk,^{a)} Jan Schroers, and William L. Johnson
California Institute of Technology, W. M. Keck Laboratory, Pasadena, California 91125

(Received 13 October 2000; accepted for publication 19 December 2000)

The critical cooling rate as well as the thermal stability are measured for a series of alloys in the Zr–Ti–Cu–Ni–Be system. Upon cooling from the molten state with different rates, alloys with compositions ranging along a tie line from $(\text{Zr}_{70}\text{Ti}_{30})_{55}(\text{Ni}_{39}\text{Cu}_{61})_{25}\text{Be}_{20}$ to $(\text{Zr}_{85}\text{Ti}_{15})_{55}(\text{Ni}_{57}\text{Cu}_{43})_{22.5}\text{Be}_{27.5}$ show a continuous increase in the critical cooling rate to suppress crystallization. In contrast, thermal analysis of the same alloys shows that the undercooled liquid region, the temperature difference between the glass transition temperature and the crystallization temperature, is largest for some compositions midway between the two endpoints, revealing that glass forming ability does not correlate with thermal stability. The relationship between the composition-dependent glass forming ability and thermal stability is discussed with reference to a chemical decomposition process. © 2001 American Institute of Physics.
 [DOI: 10.1063/1.1350624]

Alloy systems with critical cooling rates for glass formation below 100 K/s, i.e., with good glass forming ability (GFA), are a relatively recent development. Because of their resistance to crystallization, alloys such as $\text{Zr}_{41.2}\text{Ti}_{13.8}\text{Cu}_{12.5}\text{Ni}_{10}\text{Be}_{22.5}$ (Vit1)¹ and $\text{Pd}_{40}\text{Cu}_{30}\text{Ni}_{10}\text{P}_{20}$ (PCNP)² can be examined in the deeply undercooled liquid region on accessible laboratory time scales. As shown by Turnbull,³ GFA (represented by critical cooling rate) scales with the reduced glass transition temperature T_{rg} defined as the glass transition temperature T_g divided by the liquidus temperature T_l . This correlation has been confirmed in many experiments (see Ref. 4 for summary). Thermal stability in metallic glasses is usually quantified by measuring the temperature difference ΔT between the glass transition and the first crystallization event upon heating at a constant rate. For some systems, it has been demonstrated that larger values of ΔT tend to be associated with lower values of critical cooling rate R_c .^{5,6} As a result, the thermal stability has served as an indicator of GFA in these alloys.

In recent years, the crystallization of Vit1 has been extensively examined.^{7–11} Several studies of this alloy have revealed a tendency to undergo chemical decomposition in the undercooled liquid,^{7–10} which has a direct influence on the subsequent nucleation and growth of crystalline phases. Since the decomposition occurs at a temperature close to T_g , the isothermal crystallization behavior of Vit1 for low undercooling is quite different from its behavior when deeply undercooled.¹¹ In addition, a study by Schroers *et al.*¹² involving constant heating and cooling experiments has shown that Vit1 crystallizes in a different manner upon heating from the amorphous solid than upon cooling from the melt. In this study, a cooling rate of approximately 1 K/s was required to bypass crystallization during cooling, whereas a heating rate of 200 K/s was necessary to avoid crystallization of a detectable volume fraction. Chemical decomposition has also been observed in a series of alloys which lie along the tie line between

Vit1 and $\text{Zr}_{46.25}\text{Ti}_{8.25}\text{Cu}_{7.5}\text{Ni}_{10}\text{Be}_{27.5}$ (Vit4).¹³ These alloys, $\text{Zr}_{42.63}\text{Ti}_{12.37}\text{Cu}_{11.25}\text{Ni}_{10}\text{Be}_{23.75}$ (Vit1a), $\text{Zr}_{44}\text{Ti}_{11}\text{Cu}_{10}\text{Ni}_{10}\text{Be}_{25}$ (Vit1b), and $\text{Zr}_{45.38}\text{Ti}_{9.62}\text{Cu}_{8.75}\text{Ni}_{10}\text{Be}_{26.25}$ (Vit1c), show increased ΔT values compared to Vit1.¹⁴

The present work is focused on a seven alloy series which lies along the tie line described by $(\text{Zr}_{37.5+2.5x}\text{Ti}_{62.5-2.5x})_{55}(\text{Ni}_{3x}\text{Cu}_{100-3x})_{41.25-1.25x}\text{Be}_{3.75+1.25x}$, where x can vary from 0 to 25. This series includes $\text{Zr}_{38.5}\text{Ti}_{16.5}\text{Ni}_{9.75}\text{Cu}_{15.25}\text{Be}_{20}$ [Vit1(-b)], $\text{Zr}_{39.88}\text{Ti}_{15.12}\text{Ni}_{9.98}\text{Cu}_{13.77}\text{Be}_{21.25}$ [Vit1(-a)], Vit1, Vit1a, Vit1b, Vit1c, and Vit4, i.e., alloys with $x = 13$ –19, respectively. In order to determine the GFA of the alloys, continuous cooling rate experiments have been performed to establish R_c for each. These results are compared with ΔT and T_{rg} values obtained through calorimetric methods, and a chemical decomposition process in the undercooled liquid is used to explain how a disparity between GFA and thermal stability can arise in the Vit1(-b)–Vit4 alloy series.

The seven alloys in this family were prepared by arc melting elements with purities ranging from 99.5% to 99.995% in a titanium-gettered argon atmosphere. The resulting ingots were then sealed in quartz tubes under a vacuum of approximately 10^{-6} mbar, heated above the liquidus temperature, and quenched in water. A Perkin–Elmer differential thermal analyzer (DTA 7) was used to heat amorphous samples of each alloy at 10 K/min in order to determine ΔT , T_g , T_l , and the solidus temperature T_s . Continuous cooling experiments were conducted in an rf-heating device. Initially, samples with a mass of approximately 200 mg were inductively heated in a titanium-gettered argon atmosphere to 1225 K for 150 s. They were then cooled under the control of a proportional integral differential software algorithm at various rates. The experimental setup used for the continuous cooling rate measurements is detailed elsewhere.^{15,16}

Figure 1 shows some representative results of a series of continuous cooling measurements which were used to measure the critical cooling rate directly. The data were obtained by differentiating the digitally recorded temperature–time

^{a)}Electronic mail: tweniuk@its.caltech.edu

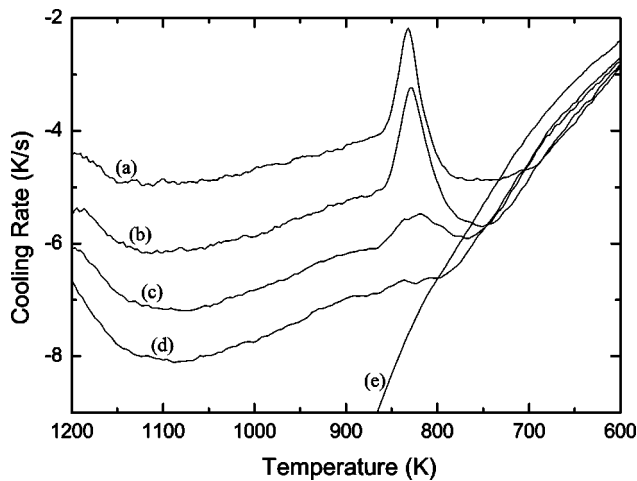


FIG. 1. Cooling rate vs temperature for Vit1b. The curves were obtained by differentiating the temperature–time profile recorded during cooling. In measurements (a), (b), and (c) an abrupt decrease in the magnitude of the cooling rate in the vicinity of 860 K marks the onset of crystallization. No crystallization peak is evident in (d). The final curve, (e), represents an experiment in which the sample was allowed to free cool from the initial annealing temperature.

profiles measured for Vit1b. For each measurement, the sample is cooled at a controlled rate from its initial temperature to some temperature below the glass transition. During cooling, crystallization in the sample manifests as an abrupt decrease in the magnitude of the cooling rate due to a release of the heat of fusion, as shown in the curves labeled (a), (b), and (c). The size of the crystallization peak decreases as the cooling rate magnitude increases in each subsequent measurement, and a crystallization event becomes undetectable, i.e., the sample has been rendered amorphous for the purposes of this study, after the cooling rate exceeds a certain value. Curve (d) represents such a measurement. Variations in cooling rate prior to crystallization can be attributed to limitations in the control algorithm used to modulate power during cooling. Thus, to determine a cooling rate value for each measurement, an average of the rate between 1200 and 900 K was calculated.

Also shown in Fig. 1 are data taken while free cooling the sample from its initial temperature. These data show another limitation of the experimental apparatus; as the temperature decreases, the maximum constant cooling rate that can be maintained decreases dramatically because the rate of heat loss from the crucible exterior limits the overall cooling rate of the sample/crucible combination. Therefore, as the constant cooling rate measurements approach the temperature where they intersect the free-cooling curve, they begin to follow the latter. In order to take measurements of cooling rates in excess of 10 K/s for Vit1c and Vit4, samples were cooled with a flow of ultrahigh purity argon. Only the downstream pressure could be varied to produce different cooling rates for samples of these alloys, and estimates of R_c have greater error as a result.

Table I lists the results of DTA scans of each alloy. For all seven alloy compositions, the glass transition temperature T_g remains essentially constant, with an average value of 625 K. The solidus temperature fluctuates to some degree, but T_l changes by a much greater amount between Vit1 and Vit4, reaching a maximum value of 1239 K in Vit1c. T_l for

TABLE I. DTA results at 10 K/min for the alloy series [Vit1(-b)–Vit4].

	T_g (K)	ΔT (K)	T_s (K)	T_l (K)	T_{rg}
Vit1(-b)	630	48	921	1003	0.628
Vit1(-a)	629	57	928	1006	0.625
Vit1	623	49	932	996	0.626
Vit1a	623	89	933	1057	0.589
Vit1b	625	114	917	1206	0.518
Vit1c	623	117	911	1239	0.503
Vit4	622	105	909	1185	0.525

Vit1, 996 K, agrees well with previous results.¹⁷

The relationship between the experimentally determined ΔT , T_{rg} , and R_c values is shown for all the alloys in Fig. 2. T_{rg} , the reduced glass transition temperature, was calculated using T_g/T_l . As shown in the top portion of Fig. 2, ΔT and T_{rg} show a negative correlation as a function of composition. Both values remain fairly constant for Vit1(-b) through Vit1 but change dramatically from Vit1a to Vit4, reaching a maximum in ΔT and a minimum in T_{rg} at Vit1c. Since T_g does not vary significantly between the seven alloys studied, this means that as ΔT increases, T_l increases as well in this alloy series.

The R_c values depicted in the lower portion of Fig. 2 show a different behavior. At one extreme, they approach a limit of approximately 1.4 K/s in Vit(-b) and Vit1(-a), but from Vit1a to Vit4 they increase steadily, reaching a maximum of 28 K/s in Vit4. The increase in R_c from Vit1a to Vit1c follows the trend toward smaller values of T_{rg} . The GFA of these alloys, however, does not seem to correlate well with the width of the supercooled liquid region, ΔT . As the critical cooling rate increases in this alloy series, the width of the supercooled liquid region also increases; those glass compositions with the largest ΔT are actually the poorer glass formers.

As shown above, the results tend to confirm Turnbull's criterion, which predicts that glass forming ability should decrease with decreasing reduced glass transition tempera-

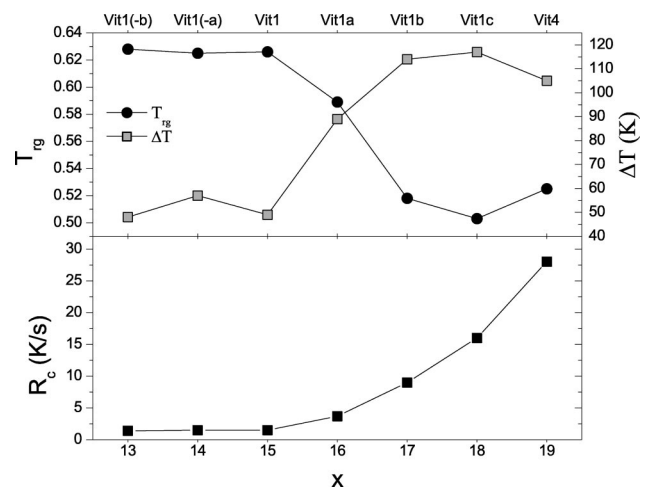


FIG. 2. Top graph shows T_{rg} and ΔT as a function of alloy composition, and bottom graph shows critical cooling rate R_c as a function of alloy composition. A dimensionless parameter x is used to represent each alloy composition in the series described by $(Zr_{37.5+2.5x}Ti_{62.5-2.5x})_{55}(Ni_{3x}Cu_{100-3x})_{41.25-1.25x}Be_{3.75+1.25x}$ along the lower horizontal axis, while the alloy designations corresponding to each x value are shown along the upper horizontal axis.

ture. However, contrary to results published for other glass forming systems, the thermal stability and GFA do not show a positive correlation for the alloy series examined in this study. This suggests that different mechanisms influence crystallization upon heating and upon cooling. It has been demonstrated that decomposition in Vit1 influences the nucleation and growth of crystalline phases in the alloy. In addition, small-angle neutron scattering research on Vit1a–Vit4 has revealed the existence of spatially correlated inhomogeneities in some of these alloys after annealing.¹³ This research has resulted in the determination of an effective critical temperature T_c for Vit1, Vit1a, and Vit1b, and has established that T_c decreases from Vit1 to Vit1c, eventually reaching the glass transition temperature between Vit1c and Vit4.

It can be expected, given the trend in critical temperature for Vit1–Vit4, that decomposition plays an important role in determining thermal stability in this alloy series (this phenomenon has also been recently observed for Zr–Ti–Cu–Ni–Al alloys¹⁸). For Vit1, the critical temperature is significantly higher (~ 60 K) than the glass transition temperature, allowing a diffusion-controlled decomposition mechanism to effect significant changes in the alloy composition during heating through the temperature range from T_g to T_c . In essence, the decomposition sets the time scale for crystallization in these alloys, increasing in amplitude until certain of the decomposed regions have a composition which favors nucleation and growth.^{8,10} For Vit1a, Vit1b, and Vit1c, the critical temperature shifts progressively lower and closer to T_g . Thus, the effects of decomposition on subsequent crystallization behavior in each alloy are mitigated by the increasingly more sluggish kinetics of each alloy at temperatures below its respective critical temperature. This results in a dramatic increase in apparent thermal stability as the time scale for the diffusion-controlled decomposition process increases. It is unclear whether T_c for Vit4 lies above or below T_g , but, given the decrease in ΔT observed between Vit1c and Vit4, it seems likely that the crystallization of Vit4 upon heating proceeds through different mechanisms than the six alloys preceding it in the series. This may also account for the abrupt increase in T_{rg} between Vit1c and Vit4 despite the fact that R_c also increases, but further study is necessary to elucidate the reasons for this departure from the Turnbull criterion. It is important to note that the critical temperature for all studied alloys is lower than the crystallization temperature measured upon cooling. Therefore, this decomposition process cannot influence the crystallization upon cooling.

In conclusion, results of continuous cooling and differential thermal analysis experiments have been presented. The critical cooling rate was directly measured with a high accu-

racy. A continuous increase in R_c and a concomitant decrease in GFA for each successive alloy in the series from Vit1(-b) to Vit4 was observed. The DTA results confirm, for the most part, the assessment of GFA for each alloy, because T_{rg} also decreases as R_c increases between Vit1 and Vit1c. The thermal stability does not follow this trend, however. ΔT values for the alloys tend to be largest for the poorest glass formers. Vit4 appears to be the exception to the observed trends in ΔT and T_{rg} , and the author speculates that a change in crystallization mechanism is responsible for the observed results for this alloy. Between Vit1(-b) and Vit1c, changes in thermal stability upon heating can be attributed to a decomposition process in the undercooled liquid. The critical temperature decreases from Vit1 to Vit1c, approaching the glass transition temperature near Vit4. As a result, crystallization upon heating is influenced directly by the time scale for decomposition in each alloy, and this time scale increases from Vit1 to Vit1c, increasing the apparent thermal stability. This decomposition process does not influence the crystallization upon cooling, which is evidenced by the fact that the critical temperature is always lower than the crystallization temperature.

This work was supported by the National Aeronautics and Space Administration (Grant No. NAG8-1744) and the Department of Energy (Grant No. DEFG-03086ER45242).

- ¹A. Peker and W. L. Johnson, *Appl. Phys. Lett.* **63**, 2342 (1993).
- ²A. Inoue, N. Nishiyama, and H. Kimura, *Mater. Trans., JIM* **38**, 179 (1997).
- ³D. Turnbull, *Contemp. Phys.* **10**, 473 (1969).
- ⁴Z. P. Lu, H. Tan, Y. Li, and S. C. Ng, *Scr. Mater.* **42**, 667 (2000).
- ⁵A. Inoue, T. Zhang, and T. Masumoto, *J. Non-Cryst. Solids* **156–158**, 473 (1993).
- ⁶T. D. Shen and R. B. Schwarz, *Appl. Phys. Lett.* **75**, 49 (1999).
- ⁷R. Busch, S. Schneider, A. Peker, and W. L. Johnson, *Appl. Phys. Lett.* **67**, 1544 (1995).
- ⁸S. Schneider, P. Thiyagarajan, and W. L. Johnson, *Appl. Phys. Lett.* **68**, 493 (1996).
- ⁹W.-H. Wang, Q. Wei, S. Friedrich, M. P. Macht, N. Wanderka, and H. Wollenberger, *Appl. Phys. Lett.* **71**, 1053 (1997).
- ¹⁰J. F. Löffler and W. L. Johnson, *Appl. Phys. Lett.* **76**, 3394 (2000).
- ¹¹J. Schroers and W. L. Johnson, *Appl. Phys. Lett.* **76**, 2343 (2000).
- ¹²J. Schroers, A. Masuhr, W. L. Johnson, and R. Busch, *Phys. Rev. B* **60**, 11855 (1999).
- ¹³J. F. Löffler, P. Thiyagarajan, and W. L. Johnson, *J. Appl. Crystallogr.* **33**, 500 (2000).
- ¹⁴C. C. Hays, C. P. Kim, and W. L. Johnson, *Appl. Phys. Lett.* **75**, 1089 (1999).
- ¹⁵J. Schroers and W. L. Johnson, *Mater. Trans., JIM* **41**, 1530 (2000).
- ¹⁶A. Masuhr, Ph.D. thesis, California Institute of Technology (1998).
- ¹⁷R. Busch, Y. J. Kim, and W. L. Johnson, *J. Appl. Phys.* **77**, 4039 (1995).
- ¹⁸J. F. Löffler, S. Bossuyt, S. C. Glade, W. L. Johnson, W. Wagner, and P. Thiyagarajan, *Appl. Phys. Lett.* **77**, 525 (2000); A. A. Kündig, J. F. Löffler, W. L. Johnson, P. J. Uggowitzer, and P. Thiyagarajan, *Scr. Mater.* (in press).